Experimental demonstration of a robust, high-fidelity geometric two ion-qubit phase gate

D. Leibfried*†, B. DeMarco*, V. Meyer*, D. Lucas*‡, M. Barrett*, J. Britton*, W. M. Itano*, B. Jelenković*§, C. Langer*, T. Rosenband* & D. J. Wineland*

* *Time and Frequency Division, National Institute of Standards and Technology, 325 Broadway, Boulder, Colorado 80305, USA*
† *Physics Department, Campus Box 390, University of Colorado, Boulder, Colorado 80309, USA*
‡ *Department of Physics, University of Oxford, Parks Road, Oxford OX1 3PU, UK*
§ *Institute of Physics, PO Box 57, 11001 Belgrade, Serbia-Montenegro*

Universal logic gates for two quantum bits (qubits) form an essential ingredient of quantum computation. Dynamical gates have been proposed[1,2] in the context of trapped ions; however, geometric phase gates (which change only the phase of the physical qubits) offer potential practical advantages because they have higher intrinsic resistance to certain small errors and might enable faster gate implementation. Here we demonstrate a universal geometric π-phase gate between two beryllium ion-qubits, based on coherent displacements induced by an optical dipole force. The displacements depend on the internal atomic states; the motional state of the ions is unimportant provided that they remain in the regime in which the force can be considered constant over the extent of each ion's wave packet. By combining the gate with single-qubit rotations, we have prepared ions in an entangled Bell state with 97% fidelity—about six times better than in a previous experiment[3] demonstrating a universal gate between two ion-qubits. The particular properties of the gate make it attractive for a multiplexed trap architecture[4,5] that would enable scaling to large numbers of ion-qubits.

A system of trapped ions interacting with laser radiation is a promising candidate for the implementation of scalable quantum information processors[1]. After demonstrations of the basic interactions necessary for quantum information processing[3,6,7], including the Sørensen–Mølmer gate[2,8] that is universal for two ion-qubits[2] and has been used to experimentally entangle two and four ion-qubits[3], our emphasis has shifted to finding reliable ways to scale this approach to many ions and to improve the fidelity of all operations. Scalability may be achieved with a multi-trap architecture[4,5,9,10]. Initial steps toward this goal with ion-qubits that are shuttled between different sub-traps were recently demonstrated[11]. In this Letter, we describe the mechanism and experimental implementation of a geometric phase gate between two ion-qubits. The infidelity of entangled states produced by the gate is about six times smaller than the best result with ions reported so far[3], making it attractive for future multi-qubit quantum information processing.

shuttling 纠缠

The quantum state $|\Psi\rangle$ of a harmonic oscillator with mass m and frequency ω can be coherently displaced in position–momentum (z, p) phase space by acting on it with a classical force $F_0 \sin(\omega t - \phi)$, resonant with the oscillator frequency[12]. If the force acts for time τ, a displacement by Δz and Δp in phase space is formally described by the action of the corresponding displacement operator on $|\Psi\rangle$ (refs 4, 12, 13):

$$D(\alpha) = \exp[\alpha a^{\dagger} - \alpha^{*} a] \text{ with } \alpha = 1/(2z_0)[\Delta z + i\Delta p/(m\omega)]$$
$$= -F_0 z_0/(2\hbar)\exp(i\phi)\tau \qquad (1)$$

where $z_0 = [\hbar/(2m\omega)]^{1/2}$ is the spread of the oscillator's ground state wavefunction. The effect of two sequential displacements $D(\alpha)$ and $D(\beta)$ is additive up to a phase factor:

$$D(\alpha)D(\beta) = D(\alpha+\beta)\exp[i\,\mathrm{Im}(\alpha\beta^{*})] \qquad (2)$$

For a suitable sequence of displacements the state $|\Psi\rangle$ can be transported around a closed loop in (z, p) phase space. The phase factors for all steps accumulate in such a way that $|\Psi\rangle$ acquires a geometric phase equal to $A/\hbar$ if the loop encloses an area A (see Methods). The acquired phase is independent of the motional state $|\Psi\rangle$. As shown below, we can use this geometric phase to realize a logic gate between two ion-qubits if the coherent driving force differs for the two logical states of the ions. In our experiments, we employ a state-dependent dipole force induced by laser light as was used to create 'Schrödinger-cat' states of a single ion[14,15].

The basic idea for this phase gate was first proposed by Milburn and is a specific case of the more general formalism described by Milburn *et al.*[16], Sørensen and Mølmer[8] and Wang *et al.*[17] For our particular experiment, the qubit logical states are two $^{9}Be^{+}$ hyperfine ground states ($|F=2, m_F=-2\rangle \equiv |\downarrow\rangle$, $|F=1,\ m_F=-1\rangle \equiv |\uparrow\rangle$). We consider a pair of ion-qubits confined together in a harmonic trap potential. The motion of the particles is strongly coupled by their mutual Coulomb repulsion and can be described in terms of normal modes. Along the direction in which the two ions are aligned in the trap (the trap axis) there are two normal modes: the centre-of-mass mode at frequency ω_c, where the displacements of both ions from equilibrium are the same, and the 'stretch' mode at frequency $\omega_s = 3^{1/2}\omega_c$, where the displacements are equal but in opposite directions.

The state-dependent displacement force is implemented with two laser beams whose frequencies (ω_1, ω_2) are detuned by $\Delta \approx +(2\pi)\times 82\,\mathrm{GHz}$ from the $2s\ ^2S_{1/2} \rightarrow 2p\ ^2P_{1/2}$ electric-dipole transition ($\lambda \approx 313\,\mathrm{nm}$) and have a relative detuning $\Delta\omega = \omega_1 - \omega_2 = \omega_s + \delta$ close to the frequency of the stretch mode ($|\omega_s| \gg |\delta|$). The electric field from the laser beams gives rise to a Stark shift of the energies of each internal state and a corresponding electric dipole force on each ion. We adjust the polarizations and frequencies of the laser beams to make the average differential energy shift between states $|\downarrow\rangle$ and $|\uparrow\rangle$ equal to zero, but on timescales $1/\Delta \ll t \ll 1/\omega_s$, there exists a different force on each state, modulated at frequency $\omega_s + \delta$. The beam directions are at right angles to each other and the direction of their wavevector difference $\Delta k = k_1 - k_2$ coincides with the trap axis. The trap potential along this axis was adjusted to fulfil the condition $\Delta k d = 2\pi p$, where d is the distance

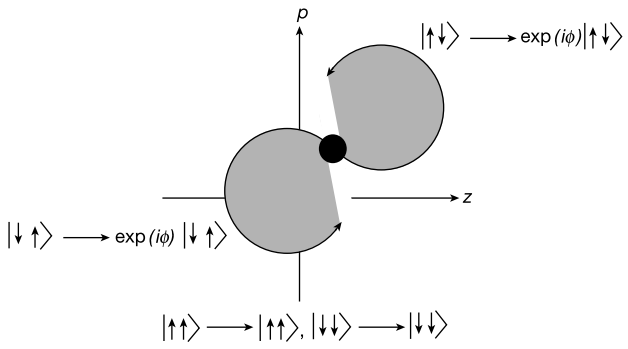

Figure 1 Phase space representation of the stretch-mode amplitude of two trapped ions. The displacement drive moves the motional state components associated with the $|\downarrow\uparrow\rangle$ and $|\uparrow\downarrow\rangle$ internal states around circular trajectories in phase space as indicated. Both components acquire the same phase because the enclosed area and sense of rotation are equal.

between the two ions and p is an integer ($\omega_s = 2\pi \times 6.1\,\mathrm{MHz}$, $\Delta k \approx 2^{1/2} \times 2\pi/(313\,\mathrm{nm})$ and $p = 9$ in the experiment). In this case, the interference pattern of the two beams has the same phase at the position of both ions. Therefore, when the ions are in the same internal state the dipole force driving each ion will be the same and no differential force arises, so the stretch mode is not excited. On the other hand, if the ions are in different internal states a differential force exists between them, exciting the stretch mode.

Owing to the detuning δ, the driving force is asynchronous with the stretch mode frequency, but re-synchronizes after a duration $T = 2\pi/\delta$. During this time the state of the motion is displaced along a circular path in phase space (see Fig. 1 and Methods), returning to the original point in phase space after time T while acquiring a geometric phase $\phi = A/\hbar$ equal to the enclosed phase space area. By choosing the intensity of the laser beams appropriately we can achieve $\phi = \pi/2$. The evolution of the wavefunction for the two ions can then be summarized by:

$$|\downarrow\rangle|\downarrow\rangle|\Psi\rangle \rightarrow |\downarrow\rangle|\downarrow\rangle|\Psi\rangle$$

$$|\downarrow\rangle|\uparrow\rangle|\Psi\rangle \rightarrow e^{i\pi/2}|\downarrow\rangle|\uparrow\rangle|\Psi\rangle$$

$$|\uparrow\rangle|\downarrow\rangle|\Psi\rangle \rightarrow e^{i\pi/2}|\uparrow\rangle|\downarrow\rangle|\Psi\rangle$$

$$|\uparrow\rangle|\uparrow\rangle|\Psi\rangle \rightarrow |\uparrow\rangle|\uparrow\rangle|\Psi\rangle = e^{-i\pi}(e^{i\pi/2}|\uparrow\rangle)(e^{i\pi/2}|\uparrow\rangle)|\Psi\rangle \qquad (3)$$

The gate is equivalent to a universal controlled π-phase gate plus $\pi/2$ individual qubit phase shifts on the $|\uparrow\rangle$ states. In a given algorithm, consisting of phase gates and single-bit rotations, additional single-qubit operations are not necessary to correct for these $\pi/2$ phase shifts, because they can be absorbed into the next single-bit rotations on the qubits in question.

The $^9Be^+$ ion-qubits are confined in a linear Paul trap[11]. State preparation is performed by stimulated Raman transitions driven by a pair of laser beams with frequency difference approximately equal to the ground-state hyperfine frequency[6]. When the frequency difference of the beams is equal to ω_S, we drive displacement transitions $|m_s\rangle|n\rangle \leftrightarrow |m_s\rangle|n+1\rangle$ (that is, $m_s \in \{\downarrow,\uparrow\}$) between oscillator number states $|n\rangle$ that give rise to the internal-state-dependent displacement. As long as the wavefunction spread and normal mode excursions are smaller than the effective wavelength $2\pi/\Delta k$ (Lamb–Dicke regime), the displacement only depends on the internal state, and not on the motional state $|\Psi\rangle$ itself[4]. In our experiment, the ratio of the extension of the stretch-mode ground-state wavefunction for one ion z_{0s} to the effective wavelength (Lamb–Dicke parameter) was $\eta_S = \Delta k z_{0s} = 0.19$. With these conditions and the value of Δ noted above we can balance the average a.c. Stark shifts on levels $|\downarrow\rangle$ and $|\uparrow\rangle$ and make $F_{0\downarrow} = -2F_{0\uparrow}$ (ref. 18).

Before each experiment all motional modes were cooled by Doppler laser-cooling, followed by 40 cycles of resolved-sideband Raman cooling that leave the centre-of-mass and stretch mode in the ground state 99% of the time[19]. The two ions were then initialized in the state $\Psi_0 = |\downarrow\rangle|\downarrow\rangle|n=0\rangle$ by optical pumping. Depending on the experiment, we applied a pulse sequence containing single ion rotations and a state-dependent displacement pulse. We then detected the internal states of both ions through state-dependent resonance fluorescence measurements[20] ($|\downarrow\rangle$ will strongly fluoresce while $|\uparrow\rangle$ will produce negligible fluorescence).

It is impossible to observe the effect of the phase gate directly, because what we can observe—the total fluorescence of the two ions—is not affected by the gate operation. Accumulated phases are most conveniently observed in an interferometer experiment. To this end we enclosed the displacement pulse between the first two pulses of a spin-echo pulse sequence acting on both ions: a $\pi/2$-pulse, followed by a delay T_s, a π-pulse, an equal delay T_s and a final $\pi/2$-pulse (see inset in Fig. 2). The spin-echo sequence was used because it makes the qubit transitions immune to the effects of time-varying frequency shifts occurring on timescales much longer than one experimental cycle ($\geq 300\,\mu s$), such as those caused by ambient magnetic field fluctuations. Because the displacement pulse and the magnetic field fluctuations are independent (the operators for these two processes commute), the pulse sequence is effectively equivalent to enclosing the displacement pulse in a $\pi/2$–$3\pi/2$ Ramsey interference experiment. The first $\pi/2$-pulse transforms the state of the ions:

$$\Psi_0 = |\downarrow\rangle|\downarrow\rangle|0\rangle \rightarrow \Psi_1 = 1/2(|\downarrow\rangle|\downarrow\rangle + |\uparrow\rangle|\uparrow\rangle + |\downarrow\rangle|\uparrow\rangle + |\uparrow\rangle|\downarrow\rangle)|0\rangle$$

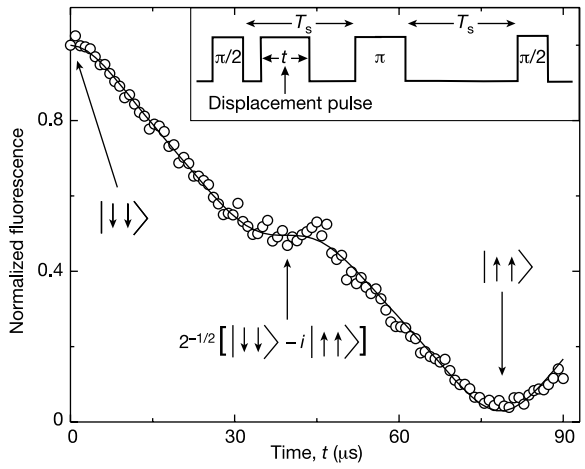

Figure 2 State evolution upon displacement. Normalized fluorescence signal (see Methods) after inserting a displacement pulse of variable duration into a spin-echo experiment that is applied to the $|\downarrow\downarrow\rangle|0\rangle$ state (see inset). The motional state returns to its point of origin after every 39 μs, leading to an approximate state $2^{-1/2}(|\downarrow\downarrow\rangle - i|\uparrow\uparrow\rangle)|0\rangle$ after 39 μs and to the approximate state $|\uparrow\uparrow\rangle|0\rangle$ after 78 μs. The solid line is a fit to the theoretically expected signal that also allows for an exponential decay in contrast with detuning and decay constant as free parameters. After 39 μs, the fitted decay constant $\tau_0 = 1.3$ ms predicts a contrast of 0.97, in good agreement with the independently determined fidelity of the entangled state produced for this gate time.

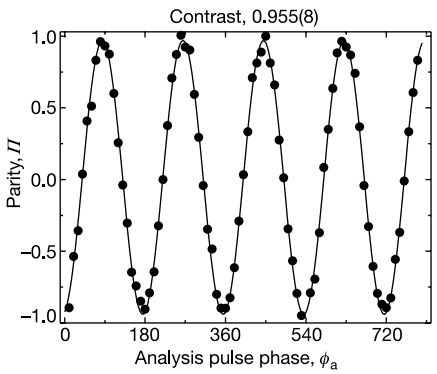

Figure 3 Parity ($[P_{\downarrow\downarrow} + P_{\uparrow\uparrow}] - [P_{\uparrow\downarrow} + P_{\downarrow\uparrow}]$) after producing the maximally entangled state. As ϕ_a is varied, the parity of the two ions should oscillate as $\cos(2\phi_a)$ with the amplitude of the oscillation equal to twice the magnitude of the density matrix element $\rho_{\downarrow\downarrow,\uparrow\uparrow}$. Each data point represents an average of 500 experimental cycles.

With no displacement pulse applied, the subsequent π- and $\pi/2$-pulses amount to just a rotation of each ion's internal state by $3\pi/2$, so the final state was $\Psi_F = |\downarrow\rangle|\downarrow\rangle|0\rangle$, leaving both ions in the fluorescing state. If the displacement pulse is applied for some time $t < T_S$ after the first $\pi/2$-pulse we expect the ions to evolve as:

$$\Psi_1 \rightarrow \Psi_2 = 1/2[(|\downarrow\rangle|\downarrow\rangle + |\uparrow\rangle|\uparrow\rangle)|0\rangle + e^{i\Phi(t)}(|\downarrow\rangle|\uparrow\rangle|\alpha(t)\rangle + |\uparrow\rangle|\downarrow\rangle|-\alpha(t)\rangle)]$$

where $\alpha(t)$ is the amplitude of the motional state displacement on the circular trajectory reached at time t, and $\Phi(t)$ is the accumulated phase (see Methods). The subsequent π- and $\pi/2$-pulses will in general return the ions not to the original state, but to a more complicated superposition state:

$$\Psi_2 \rightarrow \Psi_3 = 1/2[(|\downarrow\rangle|\downarrow\rangle + |\uparrow\rangle|\uparrow\rangle)|0\rangle + 1/2\, e^{i\Phi(t)}(|\downarrow\rangle|\uparrow\rangle - |\uparrow\rangle|\uparrow\rangle + |\downarrow\rangle|\downarrow\rangle - |\uparrow\rangle|\downarrow\rangle)|\alpha(t)\rangle + 1/2\, e^{i\Phi(t)}(|\uparrow\rangle|\downarrow\rangle - |\uparrow\rangle|\uparrow\rangle + |\downarrow\rangle|\downarrow\rangle - |\downarrow\rangle|\uparrow\rangle)|-\alpha(t)\rangle]$$

fluorescing with a rate:

$$S(t) = S_0[P_{\downarrow\downarrow} + 1/2(P_{\uparrow\downarrow} + P_{\downarrow\uparrow})] = S_0/2[1 + \exp(-|\alpha(t)|^2/2)\cos(\Phi(t))] \quad (4)$$

where S_0 is the fluorescence rate of both ions in state $|\downarrow\rangle$ and $P_{\downarrow\downarrow}$ is the probability to be in $|\downarrow\rangle|\downarrow\rangle$. If $t = lT$ (l integer) the motional state returns to its original position in phase space, that is, $\alpha(lT) = 0$, and with the intensities of the displacement pulse beams properly adjusted the accumulated phase is $\Phi(lT) = l\pi/2$. Figure 2 shows the experimentally observed fluorescence for varying lengths of the displacement pulse (circles). The fitted function (solid line) reflects the theoretical expectation (see Methods) and yields a decrease in contrast of about 3% at the proper gate pulse length of $T = 39\,\mu s$ (for $\delta/(2\pi) = 26\,kHz$).

A distinct property of quantum logic gates is that they can produce entanglement out of initially non-entangled states. In particular, inserting a proper π-phase gate pulse between the first two pulses of the spin-echo method would ideally carry out the overall transformation:

$$\Psi_0 = |\downarrow\rangle|\downarrow\rangle|0\rangle \rightarrow \Psi_P = 2^{-1/2}(|\downarrow\rangle|\downarrow\rangle - i|\uparrow\rangle|\uparrow\rangle)|0\rangle \quad (5)$$

thereby creating a maximally entangled state. The entangled nature of the state produced in the experiment can be revealed by applying a final 'analysis' $\pi/2(\phi_a)$-pulse, which has a variable phase ϕ_a relative to that of the spin-echo pulses, and deducing the parity:

$$\Pi(\phi_a) = P_{\downarrow\downarrow}(\phi_a) + P_{\uparrow\uparrow}(\phi_a) - [P_{\uparrow\downarrow}(\phi_a) + P_{\downarrow\uparrow}(\phi_a)] \quad (6)$$

from the observed fluorescence histograms[3]. The observed pattern will have a component that oscillates as $C\cos(2\phi_a)$, where $|C|$ is equal to twice the magnitude of the density matrix element $\rho_{\uparrow\uparrow,\downarrow\downarrow}$ that characterizes the coherence between the $|\downarrow\rangle|\downarrow\rangle$ and $|\uparrow\rangle|\uparrow\rangle$ components in the state produced[3]. Figure 3 shows the observed parity signal (circles) plotted versus the phase between the spin-echo pulses and the analysis pulse. The solid line is a cosine fit $C\cos(b\phi_a)$ to the observed data. The best-fit parameters give frequency $b = 1.998 \pm 0.002$ and contrast $|C| = 0.955 \pm 0.008$. Knowing the contrast of the measured interference pattern, we can directly determine the fidelity $F = \langle\Psi_P|\rho|\Psi_P\rangle = 1/2(P_{\uparrow\uparrow} + P_{\downarrow\downarrow}) + |\rho_{\uparrow\uparrow,\downarrow\downarrow}|$ of the produced entangled state with density matrix ρ. Using the populations $P_{\uparrow\uparrow} + P_{\downarrow\downarrow} = 0.98 \pm 0.02$, deduced from the histogram decomposition of our entangled-state signal[20] and $|\rho_{\uparrow\uparrow,\downarrow\downarrow}| = |C|/2 = 0.477 \pm 0.004$, the measured fidelity is $F = 0.97 \pm 0.02$. This is a lower bound for the actual fidelity of the prepared state, because it also includes the infidelity introduced by imperfect optical pumping to the initial $|\downarrow\rangle|\downarrow\rangle|0\rangle$ state and imperfect detection.

Although the phase gate is formally the same as the Sørensen–Mølmer gate[8] in a rotated basis, it has some technical advantages. For example, the phase gate has reduced sensitivity to magnetic field fluctuations, because it does not involve spin flips, as was the case for the gates demonstrated previously[3,6]. Because the displacement drive has an interaction strength that is equal to the first-sideband interactions used in the Cirac–Zoller[1] and Sørensen–Mølmer[8] gates (up to factors close to unity), the gate speed for a given laser intensity is about the same. However, for a given fidelity goal, the gate speed can be made greater than in the Cirac–Zoller and Sørensen–Mølmer gates, because the fidelity of those gates is limited by off-resonant contributions of the stronger spin-changing carrier transition[8,21] that is absent in the displacement drive (see Methods).

Like the Sørensen–Mølmer gate, individual ion addressing is not required during the gate (in any of the gates discussed, individual qubit rotations can be accomplished when the ions are spatially separated) and the accumulated phase depends only on the path area, not on the exact starting state distribution, path shape, orientation in phase space, or the time it takes to traverse the closed path. This insensitivity to the starting state means that, within the Lamb–Dicke regime, ground-state cooling is not required for accurate gate operations. The main sources of gate error in our experiment are fluctuations in δ and fluctuations in the Raman-beam intensity (both roughly at the 1% level) and a spontaneous emission probability of about 2.2% in each run of the experiment to create the state in equation (5). If frequency drift and intensity errors could be reduced to the order of 10^{-3} and spontaneous emission suppressed (by using a different ion species[18]), the expected gate infidelity is of the order 10^{-4}, the asymptotic threshold value required for fault-tolerant quantum computation[22]. The gate has an additional technical advantage over other gates in the context of quantum computing in multiplexed traps[4,5] where logic ions will be sympathetically cooled with a separate cooling ion before gate operations. In general, the normal-mode amplitudes on each ion will be different, making it technically more difficult to obtain equal laser beam couplings, as required in the Sørensen–Mølmer gate[2,3,8]. Equal coupling is not required for a general geometric phase gate because the extra phases on each qubit can be absorbed into previous or subsequent single-qubit rotations. □

Methods

Geometric phase shift

The geometric phase shift is due to coherent displacement along an arbitrary path. By dividing an arbitrary path into short straight sections $\Delta\alpha_j, j = \{1, N\}$ and repeatedly invoking equation (2), the total operation can be written as:

$$D_{total} = D(\Delta\alpha_N)\ldots D(\Delta\alpha_1) = D\left(\sum_j \Delta\alpha_j\right)\exp\left[i\,\mathrm{Im}\left\{\sum_{j=2}^{N}\Delta\alpha_j\left(\sum_{k=1}^{j-1}\Delta\alpha_k\right)^*\right\}\right] \quad (7)$$

Going to the limit of infinitesimal steps by replacing $\Delta\alpha_j$ with $d\alpha$ yields:

$$D_{total} = D\left(\int[d\alpha/d\tau]\,d\tau\right)\exp[i\Phi], \text{ with } \Phi = \mathrm{Im}\left\{\int\alpha^*(\tau)[d\alpha/d\tau]\,d\tau\right\} \quad (8)$$

If the path P is closed, then:

$$D_{total} = D(0)\exp[i\Phi], \text{ and } \Phi = \mathrm{Im}\left\{\int_P \alpha^*\,d\alpha\right\} = 1/\hbar\int_A dz\,dp = A/\hbar \quad (9)$$

In the last step we converted the path integral over P to an area integral over the area A enclosed by P, and used equation (1) to rewrite α in terms of position z and momentum p.

Expected signal for the displacement drive

For a relative detuning $\omega_s + \delta$ of the two Raman beams the infinitesimal displacement of the stretch mode amplitude at time τ is[4]:

$$d\alpha_{\uparrow\uparrow}(\tau) = -\,d\alpha_{\uparrow\downarrow}(\tau) = \Omega_D\exp[i(\phi_L - \delta\tau)]\,d\tau$$
$$d\alpha_{\downarrow\downarrow}(\tau) = d\alpha_{\uparrow\uparrow}(\tau) = 0 \quad (10)$$

where:

$$\Omega_D = -(F_{0\downarrow} - F_{0\uparrow})z_{0s}/(2\hbar) \quad (11)$$

z_{0s} is the spread of the ground-state wavefunction for one ion in the stretch mode and ϕ_L is the phase of the driving field. Evaluation of the integrals in equation (8) yields:

$$\alpha_{\downarrow\uparrow}(\tau) = i\Omega_D/\delta[\exp(-i\delta\tau) - 1]\exp(i\phi_L)$$
$$\Phi_{\downarrow\uparrow}(\tau) = (\Omega_D/\delta)^2[\sin(\delta\tau) - \delta\tau] \quad (12)$$

For the π-phase gate the maximum excursion in phase space is $|\alpha_{\uparrow\downarrow\max}| = 1$. The normalized fluorescence is equal to:

$$S_{norm}(\tau) = P_{\downarrow\downarrow}(\tau) + 1/2[P_{\downarrow\uparrow}(\tau) + P_{\uparrow\downarrow}(\tau)] = 1/2[1 + \exp(-|\alpha_{\uparrow\downarrow}(\tau)|^2/2)\cos(\Phi_{\uparrow\downarrow}(\tau))] \quad (13)$$

For the fit in Fig. 3 we allowed for an additional exponential decay:

$$S_{fit}(\tau) = 1/2[1 + \exp(-\tau/\tau_0)\exp(-|\alpha_{\uparrow\downarrow}(\tau)|^2/2)\cos(\Phi_{\uparrow\downarrow}(\tau))] \quad (14)$$

where τ_0 is a phenomenological decay constant mimicking decoherence effects.

Gate speed considerations

The gate speed in our experiments was limited by the intensity of the displacement beams. The observed ratio of gate time $2\pi/\delta$ to stretch oscillation period $2\pi\omega_S$ was 238. The largest contribution to gate infidelity from off-resonant excitations is that due to excitation of the centre-of-mass (COM) mode (as opposed to excitation of the internal-state carrier transition in the Cirac–Zoller and Sørensen–Mølmer gates). The ratio of excitation amplitude of the stretch mode to that of the COM mode scales as δ_{COM}/δ where $\delta_{COM} \propto \omega_S$ is the detuning from the COM mode. Therefore if the required fidelity restricts the COM mode excitation to be below a certain size, then the gate rate ($\propto \delta$) will scale linearly with ω_S. For our experimental parameters, we estimate the contribution to infidelity from off-resonant excitation of the COM mode to be below 10^{-4}. In a more refined scenario, we could intentionally excite both the COM and the stretch mode. For suitable parameters the COM and stretch-mode amplitudes can return to their initial values even if the gate rate exceeds the trap frequency.

Received 18 December 2002; accepted 7 February 2003; doi:10.1038/nature01492.

1. Cirac, J. I. & Zoller, P. Quantum computations with cold trapped ions. *Phys. Rev. Lett.* **74,** 4091–4094 (1995).
2. Sørensen, A. & Mølmer, K. Quantum computation with ions in thermal motion. *Phys. Rev. Lett.* **82,** 1971–1974 (1999).
3. Sackett, C. A. *et al.* Experimental entanglement of four particles. *Nature* **404,** 256–259 (2000).
4. Wineland, D. J. *et al.* Experimental issues in coherent quantum-state manipulation of trapped atomic ions. *J. Res. Natl Inst. Stand. Technol.* **103,** 259–328 (1998).
5. Kielpinski, D., Monroe, C. & Wineland, D. J. Architecture for a large-scale ion-trap quantum computer. *Nature* **417,** 709–711 (2002).
6. Monroe, C., Meekhof, D. M., King, B. E., Itano, W. M. & Wineland, D. J. Demonstration of a fundamental quantum logic gate. *Phys. Rev. Lett.* **75,** 4714–4717 (1995).
7. Roos, Ch. *et al.* Quantum state engineering on an optical transition and decoherence in a Paul trap. *Phys. Rev. Lett.* **83,** 4713–4716 (1999).
8. Sørensen, A. & Mølmer, K. Entanglement and quantum computation with ions in thermal motion. *Phys. Rev. A* **62,** 02231 (2000).
9. DeVoe, R. G. Elliptical ion traps and trap arrays for quantum computation. *Phys. Rev. A* **58,** 910–914 (1998).
10. Cirac, J. I. & Zoller, P. A scalable quantum computer with ions in an array of microtraps. *Nature* **404,** 579–581 (2000).
11. Rowe, M. A. *et al.* Transport of quantum states and separation of ions in a dual rf ion trap. *Quant. Inf. Comput.* **4,** 257–271 (2002).
12. Carruthers, P. & Nieto, M. M. Coherent states and the forced quantum oscillator. *Am. J. Phys.* **7,** 537–544 (1965).
13. Walls, D. F. & Milburn, G. J. *Quantum Optics* (Springer, Berlin, 1994).
14. Monroe, C., Meekhof, D. M., King, B. E. & Wineland, D. J. A "Schrödinger Cat" superposition state of an atom. *Science* **272,** 1131–1136 (1996).
15. Myatt, C. J. *et al.* Decoherence of quantum superpositions through coupling to engineered reservoirs. *Nature* **403,** 269–273 (2000).
16. Milburn, G. J., Schneider, S. & James, D. F. Ion trap quantum computing with warm ions. *Fortschr. Physik* **48,** 801–810 (2000).
17. Wang, X., Sørensen, A. & Mølmer, K. Multibit gates for quantum computing. *Phys. Rev. Lett.* **86,** 3907–3910 (2001).
18. Wineland, D. J. *et al.* Quantum information processing with trapped ions. Preprint quant-ph/0212079 available at ⟨http://arXiv.org⟩ (2002).
19. King, B. E. *et al.* Cooling the collective motion of trapped ions to initialize a quantum register. *Phys. Rev. Lett.* **81,** 1525–1528 (1998).
20. Rowe, M. A. *et al.* Experimental violation of a Bell's inequality with efficient detection. *Nature* **409,** 791–794 (2001).
21. Steane, A. *et al.* Speed of ion trap quantum information processors. *Phys. Rev. A* **62,** 042305 (2000).
22. Steane, A. Overhead and noise threshold of fault-tolerant quantum error correction. Preprint quant-ph/0207119 available at ⟨http://arXiv.org⟩ (2002).

Acknowledgements We thank J. Chiaverini, T. Schätz and A. Steane for comments on the manuscript. This work was supported by the US National Security Agency (NSA), the Advanced Research and Development Activity (ARDA). This is a publication of a US government agency.

Competing interests statement The authors declare that they have no competing financial interests.

Correspondence and requests for materials should be addressed to D.J.W. (e-mail: david.wineland@boulder.nist.gov).

An electronic Mach–Zehnder interferometer

Yang Ji, Yunchul Chung, D. Sprinzak, M. Heiblum, D. Mahalu & Hadas Shtrikman

Braun Center for Submicron Research, Department of Condensed Matter Physics, Weizmann Institute of Science, Rehovot 76100, Israel

Double-slit electron interferometers fabricated in high mobility two-dimensional electron gases are powerful tools for studying coherent wave-like phenomena in mesoscopic systems[1–6]. However, they suffer from low visibility of the interference patterns due to the many channels present in each slit, and from poor sensitivity to small currents due to their open geometry[3–5,7]. Moreover, these interferometers do not function in high magnetic fields—such as those required to enter the quantum Hall effect regime[8]—as the field destroys the symmetry between left and right slits. Here we report the fabrication and operation of a single-channel, two-path electron interferometer that functions in a high magnetic field. This device is the first electronic analogue of the optical Mach–Zehnder interferometer[9], and opens the way to measuring interference of quasiparticles with fractional charges. On the basis of measurements of single edge state and closed geometry transport in the quantum Hall effect regime, we find that the interferometer is highly sensitive and exhibits very high visibility (62%). However, the interference pattern decays precipitously with increasing electron temperature or energy. Although the origin of this dephasing is unclear, we show, via shot-noise measurements, that it is not a decoherence process that results from inelastic scattering events.

Direct phase measurements of electrons, customarily done in double-slit interferometers[1–4], are difficult to perform under strong magnetic fields. Electrons are diverted by the Lorentz force, perform chiral skipping orbits, and prefer one slit to the other—thus breaking the symmetry of the interferometer. At the extreme quantum limit (that is, in the quantum Hall effect, QHE, regime), the skipping orbits quantize to quasi-one-dimensional-like states, named chiral edge states. We have exploited the chiral motion of the electrons, and constructed an electronic analogue of the ubiquitous optical Mach–Zehnder interferometer[9] (Fig. 1a). A beam splitter BS1 splits an incoming monochromatic light beam from source S into two beams, which, after reflection by mirrors M1 and M2, recombine and interfere at BS2 to result in two outgoing beams (collected by detectors D1 and D2). When the phase along one of the paths varies, signals in both D1 and D2 oscillate out of phase, and as no photons are being lost, the sum of both signals stays always equal to the input, S. In the electronic counterpart (Fig. 1b), quantum point contacts (QPCs) function as beam splitters, and ohmic contacts serve as detectors. A QPC is formed in the two-dimensional electron gas (2DEG) by depositing a split metallic gate on the surface of the semiconductor and biasing it negatively with respect to the 2DEG. The induced potential in the 2DEG creates a barrier under the gate bringing the two oppositely propagating edge currents to the small opening in the barrier, thus allowing backscattering. As shown schematically in Fig. 1b, QPC1 splits the incoming edge current from S to two paths, a transmitted outer path and a reflected inner path; both later recombine and interfere in QPC2, resulting in two edge currents (collected by D1 and D2).

The actual device (Fig. 1c) was fabricated in a high-mobility 2DEG embedded in a GaAs–AlGaAs heterojunction. A ring-shaped mesa, 3 μm in width, was defined by plasma etching with ohmic contacts (for S, D1 and D2) connected to the inner and outer edges of the ring. The inner contact, D2, and the two QPCs are connected to outside sources via metallic films that hover above the surface of